PROCEEDINGS OF SCIENCE

Ground level events in association with solar and cosmic transient events

Carlos Navia[*†]
Instituto de Fisica, Universidade Federal Fluminense, 24210-346
E-mail: navia@if.uff.br

....

4th School on Cosmic Rays and Astrophysics,
August 25- September 04, 2010
Sao Paulo Brazil

[*]Speaker.
[†]This work is supported by the National Council for Research (CNPq) Brazil.

PoS(CRA School)038

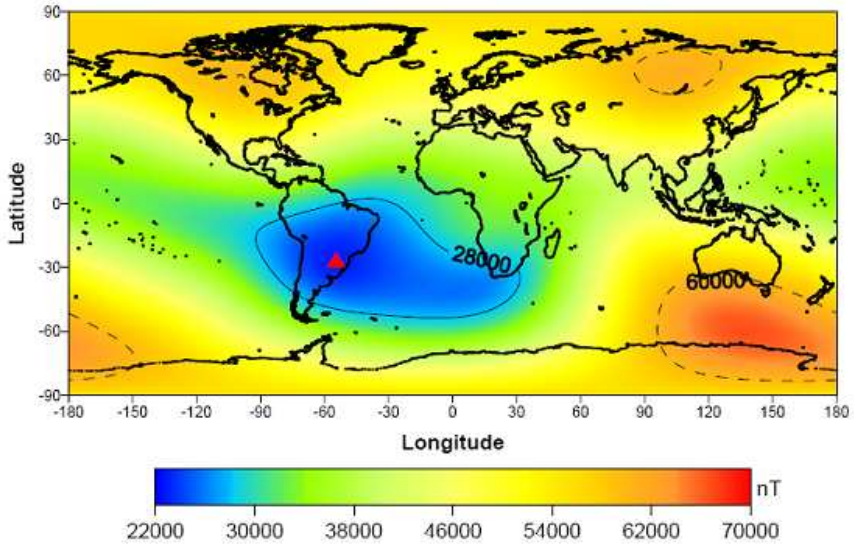

Figure 1: Geographic distribution of geomagnetic *field* intensity. The SAA boundary is around $B = 28000\ nT$. The triangle indicate the localization of the SAA's central region (26S, 53W), where the geomagnetic *field* intensity is the lowest, 22000 nT.

1. Introduction

The Earth is surrounded by the magnetosphere, which protects us from cosmic rays with energies less than several GeV by de¤ecting or capturing them in the Van Allen radiation belts. Even so, there is an additional factor that may locally enhance the cosmic ray intensity at middle latitudes. This is the so called South Atlantic Anomaly (SAA), which is an area of anomalously weak geomagnetic *field* strength with 22,000 nT in its central region (26 S, 53 W). This area covers a great part of South America's central region having magnetic *field* strength less than 28,000 nT, as is shown in Fig.1. The SAA is a result of the eccentric displacement of the magnetic *field* centre from the geographical centre of the Earth (by about 400 km) as well as the displacement between the magnetic and geographic poles of the Earth. This behaviour permits the inner Van Allen belt to impart highly energetic particles (mostly protons) which penetrate deeper down into the atmosphere owing to the low *field* intensity over the SAA, and thereby interact with the dense lower atmosphere, resulting in higher ionization and increased electrical conductivity.

In the SAA region, even incoming cosmic ray ¤uxes are higher than average ¤uxes at comparable altitudes around the world, re¤ecting an enhancement of incoming primary cosmic rays because of the SAA as well as particle precipitation

The Tupi experiment ([1]) is an Earth-based apparatus devoted to the study of cosmic rays, and is located in Niteroi City, Rio de Janeiro, Brazil, near the SAA central region. The apparatus has two telescopes. Each telescope was constructed on the basis of two detectors (plastic scintillation). One of the two telescopes has a vertical orientation, and the other is oriented near 45 degrees to the vertical (zenith), pointing to the west. Both telescopes have an effective aperture of 65.6 $cm^2\ sr$. Fig. 2 shows a photograph of the vertical telescope, and Fig. 3 shows the layout of an individual detector. The general layout of the vertical telescope, including the logic implemented in the data acquisition system using LabVIEW software, is shown in Fig. 3.

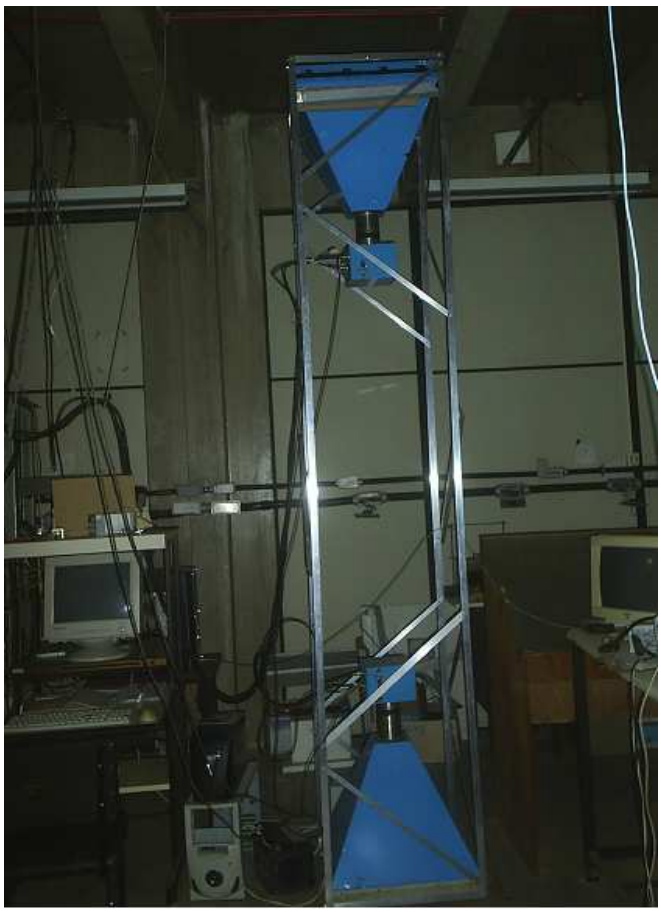

Figure 2: Photograph of the vertical Tupi telescope, located at sea level (22S, 43W) and close to the SAA central region.

The telescope counts the number of coincident signals in the upper and lower detectors. In addition, the telescope uses a veto or anti-coincidence guard system of a third detector close to the telescope. This system allows only the detection of charged particles such as muons travelling in a direction close to the vertical telescope axis. Both telescopes are inside a building under two ¤agstones of concrete, allowing registration of charged particles with energy threshold $E_{th} \geq 0.1 GeV$, which is required to penetrate the two ¤agstones.

The Tupi experiment has a fully independent power supply, with an autonomy of up to six hours to safeguard against eventual local power failures. As a result, the data acquisition is carried out 24 hours a day, giving a duty cycle greater than 90%.

Cosmic rays with an energy of around several dozens of MeV to GeV including solar particles can reach north and south polar regions, but it is dif£cult for them to reach low latitude regions due to high rigidity cut-off (above 8 GV). Nevertheless, in the SAA area, the anomalously weak geomagnetic *field* strength gives the telescopes the lowest rigidity of response to cosmic protons and ions, ($\geq$ 0.4 GV), as well as to charged secondary particles in the upper atmosphere. We report here the observation at ground of probable GeV counterparts of three small transient events. We begin with a corotating interaction region (CIR) in association with ACE solar wind spacecraft

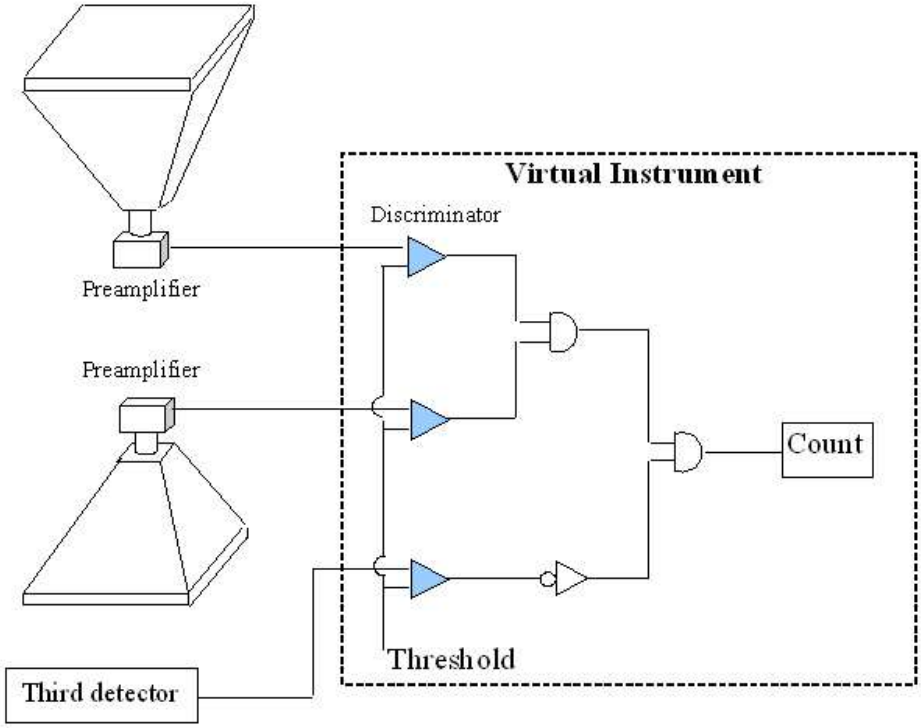

Figure 3: General layout of the vertical telescope including the logic implemented in the data acquisition system using LabVIEW software.

and a mini-¤are in coincidence with the GOES satellite to demonstrate the high sensibility of the telescopes operating in the SAA region. They constitute the smallest solar events (CIR and ¤are) detected at ground level. We then show the possible GeV counterpart of a gamma ray burst (GRB) registered by Earth orbiting Swift (BAT and XRT detectors) and Fermi (GRM) detectors.

This paper is organized as follows: In Section 2, we argue why the telescopes have a high sensitivity. The results on charged particle enhancement at ground due to a micro-¤are and two corotating interaction region are presented in Sections 3 and 4, respectively. Section 5 is devoted to showing a possible association between a ground level enhancement (charged particles at ground) and a brilliant GRB, registered by Swift and Fermi spacecraft detectors. Section 6 contains conclusions and remarks.

2. Sensitivity of the telescopes

The Earth's magnetic $field$ de¤ects the charged particles of the shower initiated by a primary particle. This de¤ection is caused by the component of the Earth's magnetic $field$ perpendicular to the particle trajectory. This effect results in a decrease in the number of collected particles and therefore in telescope sensitivity. This means that the sensibility of particle telescopes is higher in the SAA region, because in this region the magnetic $field$ strength is about three times smaller than the magnetic $field$ at the polar regions.

The radius of curvature, R, of a positive muon traveling down the atmosphere with momentum p perpendicular to the Earth's transverse magnetic $field$, $B_{(}\perp)$, is $R = p/(eB_{\perp})$. As the muon

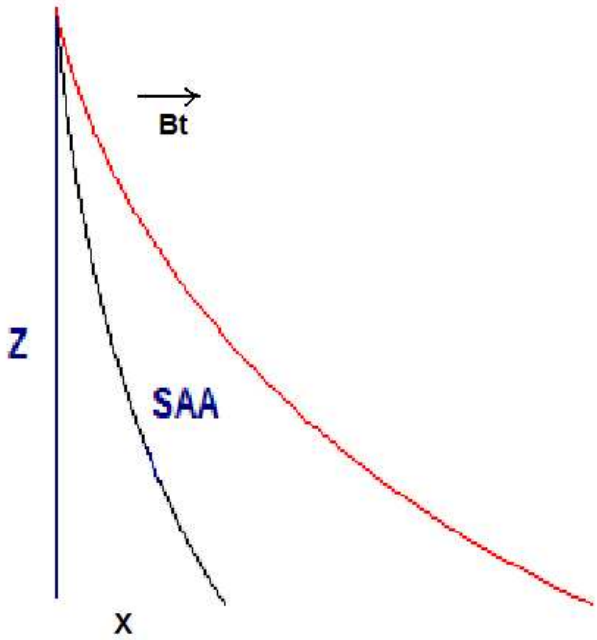

Figure 4: Comparison between the lateral shift of a vertical (born) positive muon traveling downward in the atmosphere with momentum p, due to the Earth's transverse magnetic $field$, $B_{\perp}$, inside and outside the SAA region.

travels, it will be shifted horizontally by a distance δx in the direction perpendicular to $B_{\perp}$. A relation for δx in the £rst order in z/R, where z is the height of the atmosphere where the muon is generated, can be obtained as $\delta x \sim z^2/R = z^2 ceB_{\perp}/p$. Thus the muons are shifted by a quantity that depends on the distance z but also on the momentum p of the muon. The δx in the SAA area is at least 50% smaller than the δx outside the SAA area. Fig. 4 summarizes the situation. This means that the sensitivity of the telescopes is highest in the SAA region, because the transverse magnetic $field$ is very small, even smaller than the average value for the polar regions. This offers the Tupi telescopes located in the SAA region a smaller δx and hence the highest sensitivity and the opportunity to observe small scale transient events. We have computed the magnetic $field$ (B_x, B_z) at the Tupi location and therefore the perpendicular component as a function of zenith and azimuth (θ, ϕ) ([2]).

$$\left|B_{\perp}\right|^2 = B_x^2 + B_z^2 - (B_x \sin\theta\cos\phi + B_z\cos\theta)^2. \tag{2.1}$$

The diffusion of charged particles is minimal at $\tan\theta_{min} = B_x/B_z$. The perpendicular component of the magnetic $field$ as a function of zenith and azimuth angles at the Tupi location is shown in Fig. 5. The minimum value happens at zenith and azimuth angles of $\sim 60^0$ and 0^0 respectively.

Some effects of the SAA in the cosmic ray observed at ground was shown in [3]. For instance in the Earth's upper atmosphere, there is the ionosphere (100 km above sea level) which is characterized by a larger ion concentration [4]. However, in the stratosphere at low and middle latitudes and starting from 12 km above sea level there is a residual ion concentration [5]. The ionization in this region is mainly due to cosmic rays and the effect is an increase in the stratospheric electric

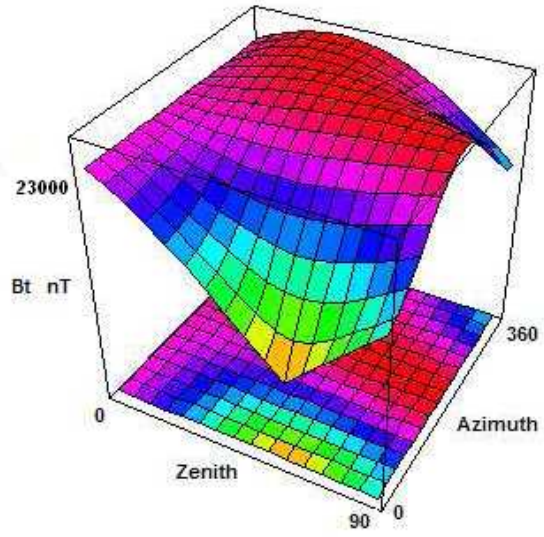

Figure 5: Perpendicular (to the vertical) component of the Earth's magnetic *field* as a function of zenith and azimuth angles at Tupi location.

conductivity, which is given by

$$\sigma = -\frac{e^2}{\nu}\sum\left(\frac{n_i}{m_i}\right), \tag{2.2}$$

where e is the electron charge, ν is the collision frequency, n_i is the ion density and m_i is the ion mass.

In the SAA region, due to the in¤uence of the lower van Allen belt, which delivers highly energetic particles (mostly protons) deeper down into the atmosphere, there is an enhancement of the ionization production and increased electric conductivity at greater atmospheric depths, and it can have one in¤uence in the longitudinal development of the a electromagnetic cascade, same which begun by a photon.

For instance, the longitudinal pro£le t_{max} of the energy deposition in an electromagnetic cascade is reasonable described by

$$t_{max} = \frac{X_{max}}{X_0} = 1.0 \times (\ln\frac{E_\gamma}{E_c} + 0.5), \tag{2.3}$$

where X_0 is the radiation length and E_c is the critical energy in air.

Due to the high electric conductivity of the SAA atmosphere, the X_0 can increase. Consequently the X_{max} also increase in the SAA region. This behavior can explain in part why in the SAA region the secondary cosmic ray intensity is higher than the world averages at the same altitude. This happen even when the primary particle is a photon.

3. Charged particle enhancements at ground in association with solar micro-¤are

A solar ¤are is de£ned as a sudden, rapid, and intense variation in brightness. A solar ¤are occurs when magnetic energy that has built up in the solar atmosphere is suddenly released. Radiation is emitted across virtually the entire electromagnetic spectrum. In solar ¤ares, the interaction

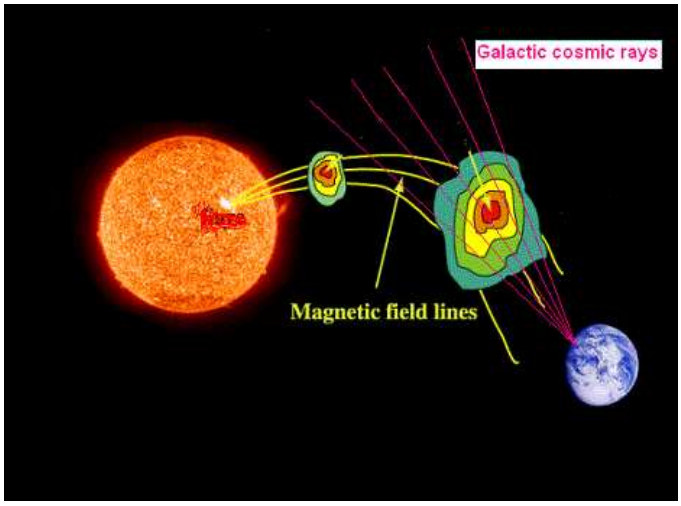

Figure 6: Diffusive transport between the Sun and the Earth of solar charged particles emitted in a solar ¤are. The effect is due to interplanetary magnetic *field* ¤uctuations, since ions (protons) have a pitch angle different from zero. Consequently, in most cases, only particles produced in very intense ¤ares will give some signal (bigger than the background produced by the cosmic rays) in the detectors located on the Earth's surface.

of the energetic electrons with thermal protons provides the deceleration, and X-ray photons with energies less than or nearly equal to the electron energy are produced. These X-ray photons are the emitted radiation signatures detected by scienti£c instruments such as GOES and SOHO. The frequency of ¤ares coincides with the 11-year solar cycle. When the solar cycle is at a minimum, active regions are small and rare and few solar ¤ares are detected. Their occurrence increases in number as the Sun approaches the maximum of its cycle. However, the period around the solar minimum is useful for the observation of small transient events, such as micro ¤ares.

Energetic particles from solar ¤ares, moving along solar magnetic *field*-lines, undergo pitch angle scattering caused by magnetic *field*-¤uctuations. This process is often assumed to be the basic physical process behind diffusive propagation of solar particles in the interplanetary space, and they are also subjected to adiabatic losses. Fig. 6 summarizes the situation, showing the diffusive transport between the Sun and the Earth of solar charged particles emitted in a ¤are. Consequently, in most cases, only particles produced in very intense ¤ares will give some signal (bigger than the background produced by the cosmic rays) in the detectors located on the Earth's surface.

Micro-¤ares (¤ares releasing $10^{27} - 10^{28} ergs$) have been identi£ed as changes in coronal emission due to impulsive heating of new materials to coronal temperature ([6, 7, 8]). The measurements of these micro events are made possible by SOHO/EIT and TRACE. The soft X-ray ¤ares classi£ed by GOES as class A ($1.0 - 9.9 \times 10^{-8} W\ m^{-2}$) are usually associated with "micro-¤ares". If the power of the ¤ares is around 10 times higher than that of micro-¤ares, they are referred to as mini-¤ares. The soft X-ray emission for solar ¤ares is a signature of the acceleration of electrons. Are there accelerated ions in these processes as well? The answers is yes, while their fraction and chemical composition as well as the relationship between ¤ares and coronal heating are still poorly

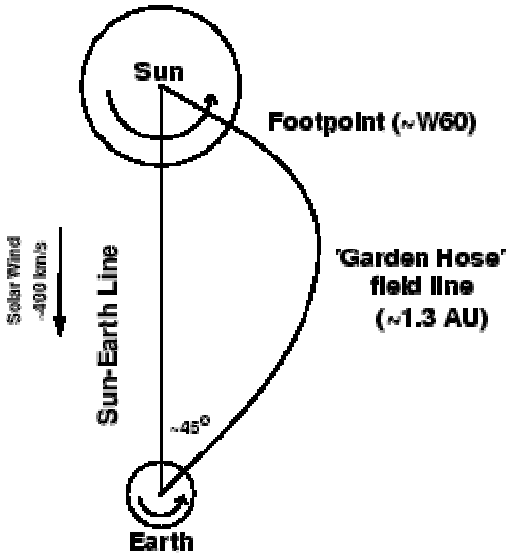

Figure 7: Example of a good magnetic *field* connection between the Sun and Earth. Flares located near to the foot-point of the "garden hose" *field* line between the Sun and Earth reach the Earth with a pitch angle close to 45^0, because, protons (ions) travel toward the Earth in a spiral trajectory, following the garden hose line and have very sharp onsets.

understood. Most of the accelerated particles should contribute to heating, and probably only a small fraction of them escape to space. In addition, it has been claimed that the micro-events have many physical properties in common with regular ¤ares, although their locations and statistical behaviours are different.

Ground-level solar ¤ares are usually observed by high latitude neutron monitors at relatively low rigidities ($\sim 1-3$ GV), and in most cases the ground-level events are linked to solar ¤ares of high intensity whose prompt X-ray emission is catalogued as X-class (above $10^4 Wm^{-2}$). Evidently, solar ¤are detection at ground level depends on several aspects, such as a good magnetic connection between the Sun and Earth. Most solar ¤ares associated with GLEs are located on the western sector of the Sun, where the IMF is well connected to the Earth. An example of a good magnetic *field* connection between the Sun and Earth is shown in Fig. 7. Flares located near the foot-point of the "garden hose" *field* line between the Sun and Earth reach the Earth with a pitch angle close to 45^0, because protons (ions) travel toward the Earth in a spiral trajectory, following the garden hose *field* line.

We show in this paper that the micro-¤ares, or at least the bigger ones (mini-¤ares), are capable of accelerating ions up to energies beyond 10 GeV, because they produce air showers in the atmosphere. These shower (charged) particles can reach up to sea level due to the high atmospheric conductivity in the SAA region.

We report here the association of charged particles enhancement in July 2010, a sharp peak in the counting rate ($E_{th} > 0.1 GeV$) observed in the vertical telescope with a signi£cance of 6.5σ, with a mini ¤are whose X-ray prompt emission is classi£ed as C-class (with a ¤ux up to $10^{-5} Watt/cm^2$) and has been reported by GOES 14. Fig. 8 summarizes the situation, where the X-ray prompt

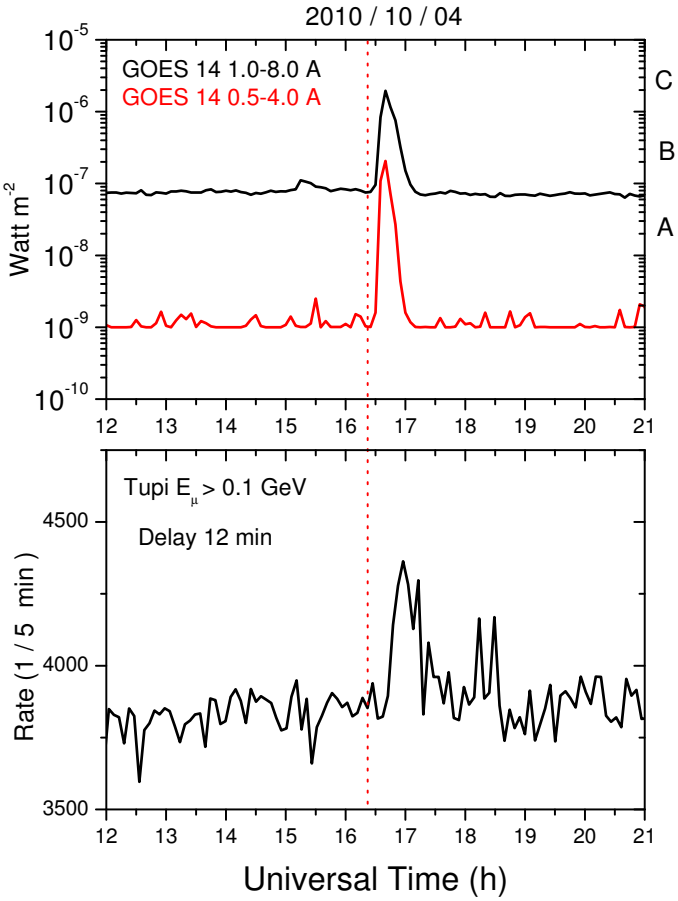

Figure 8: Top panel: The X-ray ¤ux on July 14, 2010 according to GOES 14, for two wave lengths. Bottom panel: The 5-minute counting rate in the vertical Tupi telescope. A prompt association around the 16:30 UT between a sharp peak registered by the Tupi telescope and a sudden increases in the X-ray emission (mini ¤are) registered by the Goes 14 can be observed.

emission on 14 July 2010 for two wave lengths is shown in the top panel, and the corresponding counting rate in the vertical Tupi telescope (5 minutes' binning) is shown in the bottom panel. We can see a clear association between the last X-ray enhancement observed by GOES 14 and a sharp peak in the counting rate, observed in the vertical telescope.

Now let us compare the arrival time of protons at the Earth with the time of the X-ray emission. Taking into account that the propagation time of X-ray emission is equal to 508 s.

The time delay of 12 minutes of the counting rate peak with respect to X-ray detection peak, as it is observed for this event gives us the information of a bundle of protons reaching the upper atmosphere as an almost coherent pulse, with energies above 1.0 GeV as the charged particles excess origin.

Details of this analysis as well as the association of this Tupi excess with the Fermi GBM spacecraft detector can be found in [9]

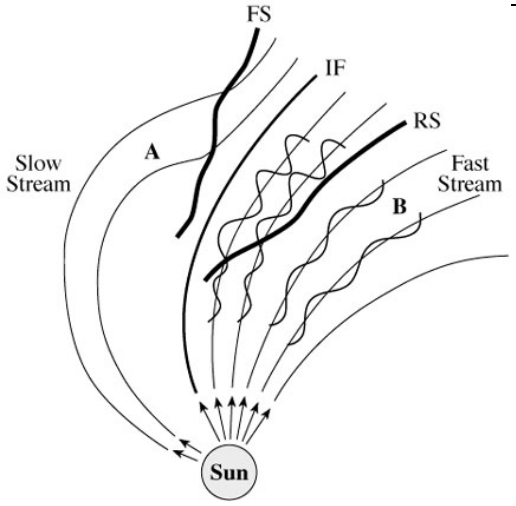

Figure 9: Mechanism of the formation of a CIR. The high-speed solar wind, originating in coronal holes, interacts with the preceeding slow solar wind, forming forward (FS) and reverse (RS) shocks.

4. Charged particle enhancement at ground due to Corotating Interaction Region

Corotating interaction regions (CIRs) are regions of compressed plasma, formed at the leading edges of corotating high-speed solar wind streams, originating in coronal holes as they interact with the preceding slow solar wind. They are particularly prominent features of the solar wind during the declining and minimum phases of the 11-year solar cycle. Fig. 9 shows the mechanism of the formation of a CIR, where the forward shock (FS) and reverse shock (RS) are regions where particles of interplanetary space are accelerated

However, in most cases, the particle enhancement observed at the ground due to a CIR occurs at a time of higher solar activity, interspersed with slow solar wind and transient ¤ows associated with coronal mass ejections (CMEs) ([10, 11]). Nevertheless, the corotating shocks that often develop at the boundaries of CIRs beyond 1 AU appear to play a role in the acceleration of interplanetary ions including cosmic rays. CIRs with developed forward and reverse shocks are occasionally observed at 1 AU. An example of corotating high-speed solar wind streams originating in coronal holes and observed on 14 July 2010 by ACE spacecraft is shown in Fig. 10 including their associated (Tupi) signal, a fall in the counting at 07:23 UT. The shock signal in the Tupi telescope has a con£dence level of 40%.

According to the CELIAS/MTOF Proton Monitor on the SOHO Spacecraft ($http://umtof.umd.edu/pm/$), the shock candidate was on 14 July 2010, at 08:20 UT, and was a reverse shock in zone 1 observed with a con£dence level of 38%. According to the Tupi register, the reverse shock £rst crossed the Earth and around one hour (57 minutes) later reached the spacecraft SOHO and ACE located at the Lagrange point L1. Starting from this delay, it is possible to calculate the average propagation speed of the shock as being $v = 410$ km/s. A clear signature of a CIR is the gradual increase in the solar wind speed.

A second example of a CIR was on 26 July 2010, at 20:30 UT, a forward shock observed by ACE spacecraft. Around 3.5 hours after, the shock was observed at the Earth by the Tupi telescope as a fall in the counting rate, Fig. 11 summarizes the situation.

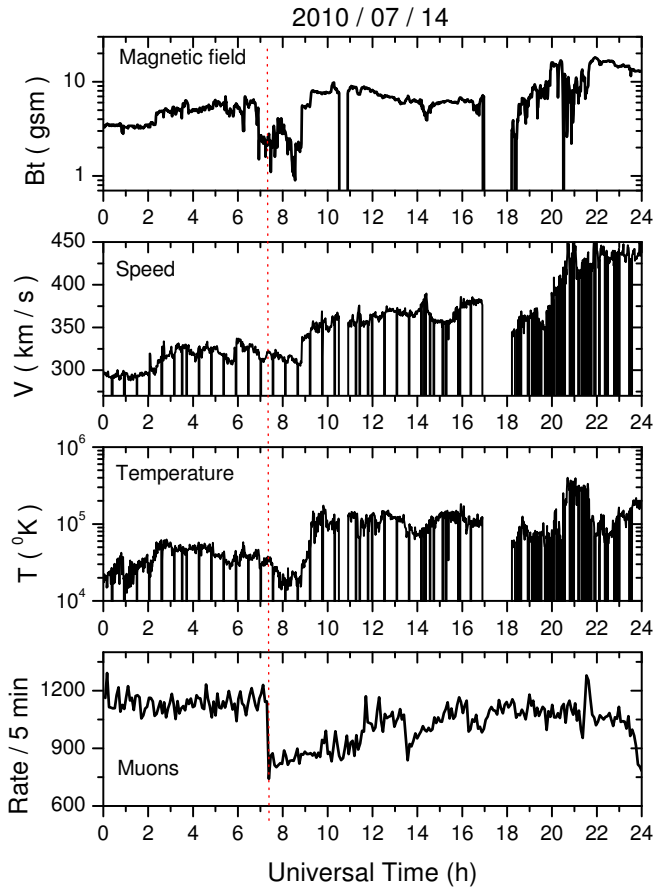

Figure 10: Example of a CIR (reverse shock) observed at 1 AU as a fall in the counting rate registered by the Tupi telescope on July 14, 2007 (bottom panel). The reverse shock crossed £rst the Earth and around one hour (57 minutes) afterwards it reaches the spacecraft ACE located in the Lagrange point L1. A clear association between the Tupi signal (reverse shock) and the ACE solar wind parameters such as magnetic *field* B_t, speed, and temperature can be observed.

5. Ground level enhancement in association with a gamma ray burst

Since their discovery by an American military satellite (the Vela project) in 1967, GRBs have evoked intense interest in the scienti£c community, because they are the most energetic explosions in the universe. Typical GRBs detected by satellite borne detectors are constituted by keV to MeV photons and they have energy ¤uxes from 10^{-6} to 10^{-4} *erg* cm^2, varying in intensity over time scales from milliseconds to several dozens of seconds. EGRET, on board the Compton Gamma Ray Observatory (CGRO), has shown that the high energy (MeV-GeV) GRB emission lasts longer than the keV emission. There were at least £ve long EGRET GRBs detected simultaneously with bright BATSE sub-MeV emissions ([12, 13, 14, 15]). These MeV-GeV long duration EGRET emissions arrive at the detector in fragments, and they are delayed or anticipated with respect to the keV-MeV BATSE bursts. Nevertheless, it is not clear how high in energy this long duration component extends, even though many models ([16, 17, 18]) predict a ¤uence in the GeV-TeV range that is comparable to that at keV-MeV scales.

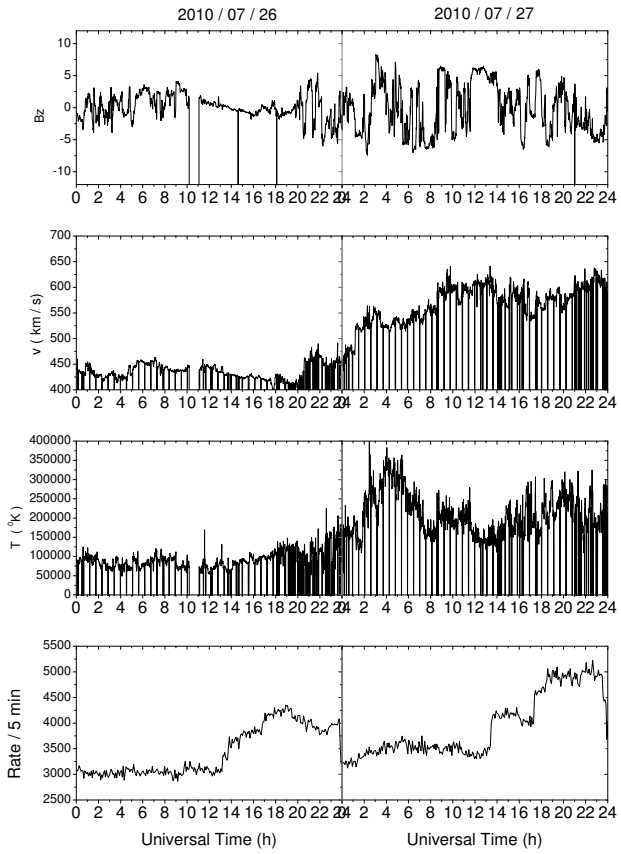

Figure 11: The same as *figure* 10., for the case of a CIR on 26 July 2010

There have been other detections of high energy GRB emissions, such as GRB 080514B detected by the AGILE gamma-ray satellite ([19]). This was the £rst GRB, after EGRET, where photons of more than several tens of MeV have been detected. Recently, the Fermi LAT instrument has detected eight GRBs at energies above 100 MeV ([20]), including the extreme GRB080916C (GCN Circular 8246) whose analysis is available at ([21]). This GRB shows that the emission above 100 MeV lasts 20 minutes longer than the emission seen with the Fermi GBM in the low energy region. In addition, the GRB LAT emission is delayed with respect to the GBM emission.

At ground level, with the exception of the evidence for TeV emission from BATSE GRB 970470 observed by Milagrito ([22]), a water Cherenkov experiment and a prototype of the Milagro experiment, no conclusive emission has been detected for any single GRB above 100 GeV. For instance, there were ~ 42 satellite-triggered GRBs within the *field* of view of MILAGRO ([23]) but no signi£cant emission was detected from any of these bursts. A similar result has been reported by the ARGO project, a large area detector ($70 \times 70 m^2$) installed in Tibet ([24]), as well as the LAGO Project ([25]), a grid of water Cherenkov detectors at mountain altitudes. This result is an indication of strong absorption of high-energy gamma rays by the extragalactic background light or perhaps, in part, by the atmospheric absorption of air shower particles initiated by a gamma ray of ~ 100 GeV. In order to minimize the atmospheric absorption, the High Altitude Water Cherenkov

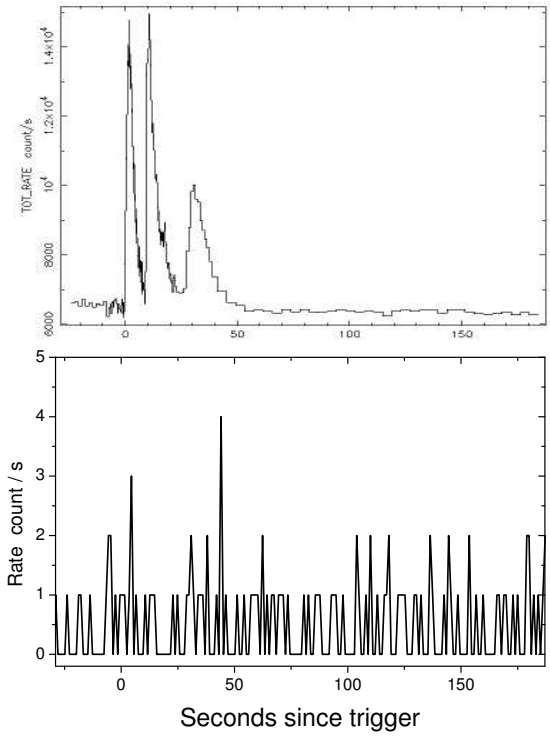

Figure 12: Top panel: The light curve of the Swift GRB 100615A (BAT trigger 424733). Bottom panel: The counting rate in the vertical Tupi telescope. We can see a peak with a signi£cance level of 4.3σ, within the coincidence time window $1 \times \Delta T_{90}$ of the burst.

(HAWC) project represents the next generation of water Cherenkov gamma ray detectors at extreme altitude ($>$ 4km asl)([26]).

The search for a transient event such as a burst signal in the Tupi telescopes is done in the scaler mode, where the single hit rate is recorded once every one second. In the scaler mode, a transient event such as a GRB is detected through the charged particles that survive in the photon air shower.

So far, there are three charged particle enhancements registered by the Tupi telescopes as candidates for a counterpart to GRBs: the GRB090315 (Hurley et al., GCN Circular 9009), the Fermi GRB100330309 (submitted to Phys. Rev. D), and the present event Swift GRB 100615A (BAT trigger 424733). This present event is catalogued as a GRB (D' Elia et al. GCN Cir. 10841), and it is a multi-peak event with a duration of $\sim$ 60 seconds, with a rate signi£cance of 24.87σ and an image signi£cance of 10.47σ. It is a brilliant GRB. This event has also been observed by Fermi GBM (Foley et al. GCN Cir. 10851) and catalogued as a GRB with a probability of 100% by the GBM ¤ight software. However, this GRB was not observed by the Fermi LAT detector designed to observe photons with energy above 100 MeV. However, only $\sim$ 10% of the Fermi GBM-GRBs, within the LAT *field* of view, gave some signal in the Fermi LAT detector.

The Swift trigger time was at 01:59:03 UT, and the light curve consists of three peaks with a duration (T_{90}) of about 50.0 s, as shown in Fig. 12 (top panel), and coincides with Tupi telescope onset time. This GRB event correlates temporally with a charged particle enhancement, a probable GeV counterpart of this burst observed at ground level (sea level) by the Tupi tilted telescope. The

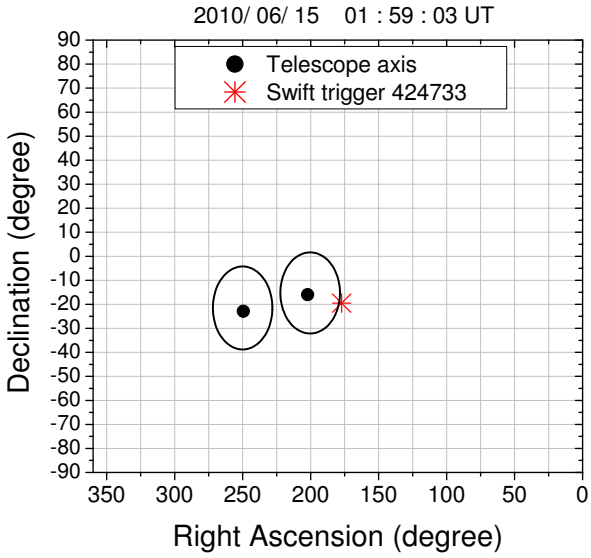

Figure 13: Equatorial coordinates showing the position of the two telescopes axis. The ellipses represent the *field* of view of the telescopes, and the asterisk is the position of the Swift trigger 424733 coordinates.

counting rate (1 Hz) presents a peak (charged particle excess) with a signi£cance level of 4.3σ and is within the coincidence time window $1 \times \Delta T_{90}$ of the burst as is shown in Fig. 12 (bottom panel). In addition, the GRB coordinates are within the *field* of view (just in the periphery) of the vertical Tupi telescope. Fig. 13 summarizes the situation, showing the telescope axis equatorial coordinates together with the GRB 100615A coordinates. The "ellipses" represent the *field* of view (FoV) of the telescopes.

We have calculated the Poisson probability P_i of a signal (counting rate enhancement) being background ¤uctuation in the time window of $\Delta t = 1s$. Fig. 14 shows the cumulative Poisson distribution of P_i obtained during the time (1.98 h) in which the GRB coordinates are inside of the *field* of view of the tilted telescope. The solid line is the expected distribution under an assumption of no signal. In this plot, the cluster of points with very low probabilities is substantially separated from the statistical background, represented by clusters to the right of the straight line. In addition, clusters to the left of the straight line represent true particle enhancements and in most cases are produced by particle precipitation in the SAA. From this analysis, we can conclude that the probability of the charged particle excess in association with the GRB 100615A being a background ¤uctuation is estimated to be $\sim 1\%$. The probability of it representing particle precipitation in the SAA (mostly energetic protons) coming from the inner Van Allen belt is estimated to be $P_i = 0.04$.

If we assume the GRB has a power law photon spectrum $dN_\gamma/dE_\gamma \propto E_\gamma^{-\beta}$ in the GeV-TeV energy range, with index $\beta \geq 2$ is possible to estimate, starting from the data of the GLE, the upper ¤uence in the 10 GeV to 1 TeV as $5.4 \times 10^{-6}\ erg/cm^2$. This result is close to the ¤uence of the £ve EGRET GRBs (100 MeV-5 GeV) whose average ¤uence is $7.2 \times 10^{-6} erg/cm^2$ observed as a counterpart of BATSE GRBs ($> 20keV$) with an average ¤uence of $2.6 \times 10^{-4} erg/cm^2$.

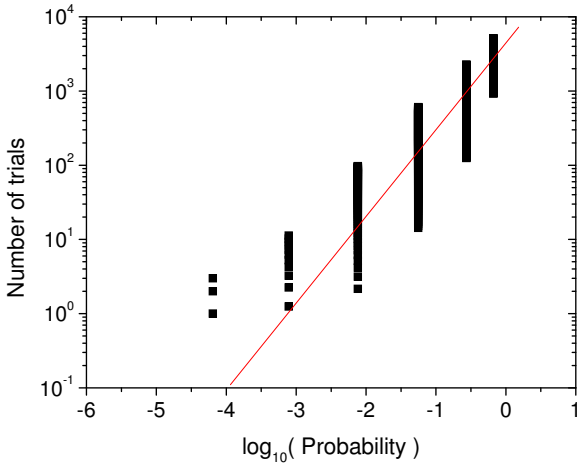

Figure 14: Cumulative distribution of the Poisson Probability P_i of a signal to be a background in the time window of $\Delta T = 1$ s, obtained during the time (1.98 h) in which the GRB coordinates are inside the *field* of view of the tilted telescope. The solid line is the expected distribution under the assumption of no signal.

6. conclusions

The shielding effect of the magnetosphere is lowest in the SAA region and the Tupi telescopes are within this region and close to its centre. This characteristic is useful for the observation of small transient events such as Solar Flares and GRBs. In fact the primary charged particles as well as the secondary charged particles come deeper down into the atmosphere owing to the low *field* magnetic intensity over the SAA. In addition, the high conductivity of the atmospheric layers in the SAA region due to particle precipitation favours the propagation of secondary charged particles originated by small transient events (increasing their range). However, the precipitation of particles in the SAA introduces an additional noise and it can mask true events.

In order to show the telescope sensitivity to gamma ray burst, we have £rst presented three small solar transient events: a mini solar ¤are and two CIRs, Previously, particles coming from such events had only been observed through spacecraft instruments. The existence of a high energy counterpart of these events at ground comes from charged particles observation. That is to say, it is necessary to have primary particles with energies above the pion production threshold, to produce air showers (particles) in the atmosphere and at least a fraction of them can reach up to sea level, due to SAA conditions.

We believe that these considerations are also valid for the GeV counterpart observed as "charged particles excess" in association with the gamma ray burst GRB100615A. However, the photon-air cross section for pion production is around 500 times smaller than the proton-air cross section for pion production in the same energy region. Consequently the channel $\gamma \rightarrow e^+e^-$ probably is dominant in the photon air shower.

Charged particle excess at ground due to a GRB requires photon energies above 10 GeV for the detection of charged particles with an energy threshold of 0.1 GeV. The search for gamma ray burst signal in the Tupi telescopes is done in the scaler mode, where the single hit rate is recorded once every one second. In the scaler mode, a transient event such as a GRB is detected through

the charged particles that survive in the photon air shower. In addition, the detection of a GRB by the Tupi telescopes requires that the GRB coordinates be within the *field* of view of the telescope where the muon excess has been found.

Finally, from a con£dence analysis, we conclude that the probability of the muon excess in association with the GRB 100615A being a background ¤uctuation is estimated to be $\sim 1\%$. The probability of it representing particle precipitation in the SAA (mostly energetic protons) is estimated to be $P_i = 0.04$. So far, there are at least three muon enhancements observed by the Tupi telescopes, with strong characteristics suggesting that they are considered as GeV counterparts of GRBs. In all these cases, they have a ¤uence in the range 10^{-6} erg/cm^2. An overview of these observations will be presented in a separate paper.

Acknowledgements This work is supported by the Brazilian National Council for Research (CNPq), under Grants No. $479813/2004-3$ and $476498/2007-4$. We are grateful to various catalogs such as ACE Science Center and the Gamma-ray bursts Coordinates Network (GCN) available on the web and to their open data policy.

References

[1] Augusto, C. R. A., Navia, C. E., and Tsui, K. H., Phys. Rev. D,77, 123008 (2008)

[2] R. de los Reyes et al., Inter. J. of Moder. Phys. A20, 7006 (2005)

[3] Augusto C. R. A. et al., Astroparticle Phys., 34, 40 (2010)

[4] Mitra, s. K., Nature, 142, 914 (1938)

[5] Gupta, S. P., Advances in Space Research, 34, 1798 (2003)

[6] Krucker, S. and Benz, A. J., Astrophys. J., 501, L213 (1998)

[7] Berghmans, D., Clette, F. and Moses, D., Astr. and Astrohys 336, 1039 (1998)

[8] Aschwand, M. J. et al., Astrophys. J., 535, 1027 (2000)

[9] Augusto, C. R. A., et al., arXiv:1012.1561v1 [astro-ph.SR]

[10] Iucci, N., Parisi, M., Storini, M. and Villoresi, G., Il Nuovo Cimento 2C, 421 (1979)

[11] Richardson, I. G., Cane, H. V. and Cliver, E. W., 2002 J. Geophys. Res. 107, 10.1029/2001JA000504.

[12] Sommer, M. et al., Astr. Phys. J., 422, L63

[13] Dingus, B., L., Astr. Phys. Esp. Scien., 231, 187 (1995)

[14] Schneid, E. et al. Astr. and Astrophys., 255, L13 (1992)

[15] Hurley, K., et al., Nature, 372, 652 (1994)

[16] Totani, T., Astropart. Phys., 11, 451 (1999)

[17] Dermer, C. D. et al., Astrophys. J , 537, 785 (2000)

[18] Pilla, R. P., and Loeb, A., Astr. Phys. J., 494, L167 (1998)

[19] Guiliani et al.,Astr. and Astrohys., 491, L25 (2008)

[20] Omodei, N., et al., Pre-Print arXiv.0907.0715 v1

[21] Abdo, A. A., et al., Science, 323, 1688 (2009)

[22] Atkins, A., et al., Astrophys. J., 533, L119 (2000)

[23] Abdo, A. A., et al., Astrohys. J., 666, 361 (2007)

[24] Di Sciascio, G and Di Girolamo, T., Astrophys. Space. Sci., 309, 537 92007).

[25] Allard., D., et al., Nuc. Inst. and Meth. in Phys. Research, A 595, 70 (2008)

[26] Huntemeyer, P., Matthews, J., Dingus, B., To appear in Proceedings of the 31th ICRC Lodz 2009